International Journal of Research in Engineering, Science and Management
Volume 8, Issue 3, March 2025
https://www.ijresm.com | ISSN (Online): 2581-5792

Critical Assessment of Containership Motions in Time Domain

Olusegun Samuel Dare[1*], Eferebo Sylvanus Ibietela[2]
[1]Lecturer I, Department of Marine Engineering, Nigeria Maritime University, Okerenkoko, Delta State, Nigeria
[2]CEO, Somatrix Marine Limited, Abuja, Nigeria

Abstract*: This study investigates the time-domain motion response of a containership to wave excitation using the Boundary Element Method (BEM). Accurate prediction of ship motions is crucial for safe and efficient maritime operations. This research focuses on a comprehensive analysis of the vessel's six degrees of freedom (surge, sway, heave, roll, pitch, and yaw) to understand its dynamic behavior in realistic sea conditions. A 3D model of the containership hull, derived from a SolidWorks-generated STL file with a surface area of 12,569,830,985.5274 mm² and overall dimensions of 213078.4316 mm (X), 36049.9816 mm (Y), and 16344.666 mm (Z), serves as the geometric basis for the BEM calculations. The time-domain BEM approach allows for a detailed examination of the vessel's transient and steady-state responses to wave forces. The analysis encompasses the computation of wave-induced forces, added mass, and damping coefficients, which are then incorporated into the vessel's equations of motion. The study presents time histories of displacement, velocity, and acceleration for each motion mode. Key findings reveal significant motion amplitudes in surge, sway, and heave, with peak displacements reaching approximately 0.5m, 0.1m, and 0.5m, respectively. Rotational motions, while smaller in displacement, exhibit significant velocities and accelerations, particularly in pitch and yaw. Specifically, yaw velocity and acceleration reach substantial values of approximately 2000 rad/s and ±2000 rad/s², respectively, highlighting the critical role of stabilization systems. The results emphasize the importance of considering all six degrees of freedom in ship motion analysis. The identified critical motion modes and their associated peak values provide crucial information for optimizing ship design, enhancing stability, and ensuring safe operation in challenging sea environments. This study demonstrates the effectiveness of the time-domain BEM in capturing the complex hydrodynamic interactions and providing valuable data for improving vessel performance and safety.

***Keywords*: Containership Motions, Time Domain Analysis, Hydrodynamics, Motion Prediction, Boundary Element Method (BEM), Potential Flow, Surge, Sway, Heave, Roll, Pitch, Yaw, Six Degrees of Freedom (6DOF), Wave-Structure Interaction, STL File, Hull Surface, Added Mass, Damping Coefficients.**

1. Introduction

The study of containership motions in the time domain is critical for understanding vessel dynamics, optimizing operational efficiency, and ensuring safety in maritime transportation. Containerships, which form the backbone of global trade by carrying vast amounts of cargo across oceans, are subjected to complex environmental forces, such as wave-induced excitations, wind loads, and varying sea states. These forces lead to vessel motions—namely surge, sway, heave, roll, pitch, and yaw—which can significantly impact cargo integrity, fuel efficiency, and crew safety if not effectively managed [1], [2].

Time-domain analysis offers a detailed and realistic representation of ship motion responses compared to frequency-domain methods, as it allows for the simulation of transient effects, nonlinear behaviors, and varying environmental conditions [3]. This approach leverages numerical methods, such as the Boundary Element Method (BEM) and computational fluid dynamics (CFD), to solve hydrodynamic equations and assess the vessel's response under time-varying wave forces. Time-domain simulations have become increasingly relevant for modern containership designs, as they enable predictions of critical phenomena such as parametric roll, slamming, and wave-induced vibrations, which can jeopardize vessel stability and cargo safety [4].

The critical assessment of containership motions in the time domain is essential for evaluating motion amplitudes, accelerations, and associated forces during real-world operations. This study provides insights into improving vessel design, optimizing loading configurations, and implementing effective stabilization mechanisms to mitigate excessive motions. Furthermore, with advancements in computational techniques and high-performance computing, time-domain methods are now more accessible, enabling a deeper understanding of containership behavior under dynamic sea conditions [5]. This research contributes to addressing the challenges of motion-induced cargo damage, fuel inefficiency, and operational safety, supporting the development of more resilient and efficient maritime transportation systems.

2. Literature Review

The study of containership motions in the time domain has garnered significant attention in marine hydrodynamics due to its critical role in ensuring vessel safety, operational efficiency, and cargo integrity. The six degrees of freedom (surge, sway, heave, roll, pitch, and yaw) associated with ship motions result from external forces such as wave excitations, wind, and

*Corresponding author: olusegunsamuel252@yahoo.com

varying sea states. A robust understanding of these dynamic responses is essential to mitigating adverse effects, including parametric roll, slamming, and resonance [1], [2]. While early research primarily relied on frequency-domain approaches, time-domain methods have emerged as a more comprehensive solution, capturing transient responses and nonlinear phenomena often overlooked in linear frequency-domain analyses [5], [4].

Time-domain analysis enables detailed simulations of ship motion under irregular and dynamic wave conditions. Numerical methods, such as the Boundary Element Method (BEM), have been widely adopted for solving hydrodynamic forces and predicting vessel responses. [1] highlighted the advantages of BEM in analyzing wave-body interactions, where Green's functions and potential flow theory serve as the foundation for hydrodynamic computations. Recent studies, such as [4], extended these approaches by incorporating nonlinear wave loads and hull interactions, providing greater accuracy in assessing ship motions, particularly in rough seas.

Further advancements have been driven by Computational Fluid Dynamics (CFD), which offers higher fidelity for complex scenarios involving viscous effects, wave-breaking, and large-amplitude ship motions [6], [7]. CFD simulations complement traditional BEM-based methods by resolving fluid-structure interactions, although at higher computational costs. For example, studies comparing CFD and potential-flow-based BEM solutions demonstrate that while BEM remains efficient for linear and quasi-linear problems, CFD excels in nonlinear and extreme wave conditions [8], [4]. These methods are particularly relevant for containerships, which are prone to phenomena like parametric roll and slamming during heavy seas due to their unique hull geometry and cargo distributions [9].

A critical challenge in containership motion analysis is the accurate prediction and control of roll motions, which have been extensively studied due to their impact on vessel stability. Parametric roll, a nonlinear phenomenon that occurs under certain wave conditions, can result in excessive roll amplitudes and loss of cargo integrity. [5] and [6] demonstrated that time-domain simulations effectively capture the onset and progression of parametric roll compared to frequency-domain methods. These findings have been further validated through experimental studies and full-scale sea trials, emphasizing the importance of coupling numerical results with physical validation.

The role of time-domain simulations in optimizing vessel performance has also been explored in the context of energy efficiency and operational planning. [4] illustrated that accurate time-domain analysis aids in assessing fuel consumption under varying sea states, allowing operators to adjust speed and heading to minimize resistance and fuel costs. Such analyses are critical in meeting regulatory requirements for energy efficiency, such as the International Maritime Organization's Energy Efficiency Design Index (EEDI) standards.

The literature underscores the significance of time-domain analysis in assessing containership motions, with methodologies like BEM and CFD playing pivotal roles. While BEM offers efficiency in linear and moderately nonlinear problems, CFD provides the accuracy needed for extreme scenarios, albeit at higher computational demands. Continued integration of numerical methods with experimental data is essential for enhancing the reliability of ship motion predictions, ensuring safety, and improving operational efficiency in global maritime transportation.

3. Methodology

A. Coupling with Numerical Time-Domain Solvers

In the time domain, hydrodynamic forces are often represented using convolution integrals, combining the radiation forces with retardation functions, while the diffraction forces are directly derived from incident wave conditions. This approach ensures accurate modeling of transient responses in vessel dynamics [10].

Where φ is the complex amplitude of the potential $\emptyset$, and they both satisfy the Laplace Equation (1).

$$\nabla^2\emptyset = 0 \; and \; \nabla^2\varphi = 0 \tag{1}$$

Our purpose is to solve the frequency domain potential function φ . Firstly, the total potential φ (Equation (2) is considered as the sum of three components. Incoming wave, scattered wave and radiated wave; and all three potentials satisfy the Laplace condition according to Equation (3) [11] and [12].

$$\varphi = \varphi_o + \varphi_s + \varphi_R \tag{2}$$

$$\nabla^2\varphi_o = \nabla^2\varphi_s = \nabla^2\varphi_R = 0 \tag{3}$$

Where, φ_o is the potential of the incoming wave, $\varphi_s$is the potential of the scattered wave due to the existence of the marine structure, $\varphi_R$is the potential of the radiated wave. The fluid domain of interest is enclosed by the body surfaceS_b, the free surface, S_f the seabed S_z and the control surface S_c as shown in Figure 1.

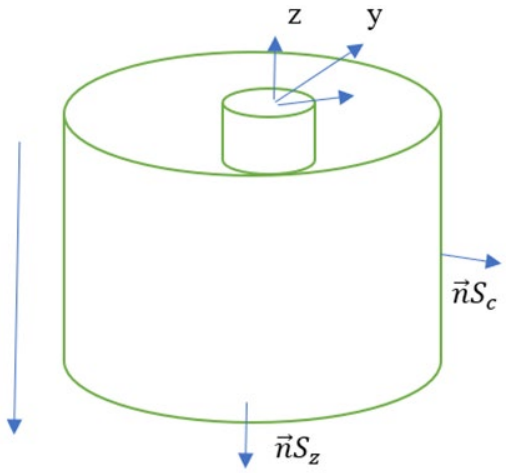

Fig. 1. BEM Fluid domain of interest

Free Surface S_f linearized free surface boundary conditions represented as Equations (4) to (6) for incident, scattered and radiation potentials respectively;

$$\frac{\partial \varphi_o}{\partial z} = K\varphi_o \tag{4}$$

$$\frac{\partial \varphi_s}{\partial z} = K\varphi_s \; when \; z = 0 \tag{5}$$

$$\frac{\partial \varphi_R}{\partial z} = K\varphi_R \tag{6}$$

Linearized free surface boundary condition according to Equations (7) or (8),

$$\frac{\partial^2 \varphi}{\partial t^2} + g\frac{\partial \varphi}{\partial z} = 0 \tag{7}$$

$$\frac{\partial^2 \varphi}{\partial t^2} = -\omega^2 \varphi \tag{8}$$

Where $K = \frac{\omega^2}{g}$

The Seabed S_z: Seabed boundary Conditions are captured as Equations (9), (10) and (11) for incident, scattered and radiation potentials respectively.

$$\frac{\partial \varphi_o}{\partial_z} = 0 \tag{9}$$

$$\frac{\partial \varphi_s}{\partial_z} = 0 \; when \; z = -h \tag{10}$$

$$\frac{\partial \varphi_R}{\partial_z} = 0 \tag{11}$$

Based on the free surface seabed conditions, the velocity potential for incoming wave can be solved using Equations (12) for for deep water when $h > \frac{\lambda}{2}$,

$$\varphi_o = \frac{igA}{\omega} e^{kz - ikx\cos\beta - iky\sin\beta} \tag{12}$$

Within the fluid domain, we suppose there are two velocity potential functions which satisfy the Laplace condition of Equation (1).

The target potential function φ, known as potential function $\emptyset_o$ for instance, the potential for the green function or the Rankine source and suppose both functions satisfy the Laplace Equation (1) that is

Using the gauss divergence theorem, we have the enclosed volume v as Equation (13).

$$\oiint_{S_c+S_b+S_f+S_z} \left(\varphi \frac{\partial \emptyset_o}{\partial n} - \emptyset_o \frac{\partial \varphi}{\partial n}\right) ds = \iiint_v \nabla(\varphi \nabla \emptyset_o - \emptyset_o \nabla \varphi) dv \tag{13}$$

Where $v = S_c + S_b + S_f + S_z$

So, if we simplify the left-hand side of Equation (13) and Equate it to zero, we have Equation (14) and (15).

$$\iiint_v \nabla(\varphi \nabla \emptyset_o - \emptyset_o \nabla \varphi) dv = \iiint_v (\nabla.\varphi.\nabla.\emptyset_o + \varphi \nabla^2 \emptyset_o - \nabla.\emptyset_o.\nabla.\varphi - \emptyset_o \nabla^2 \varphi) dv \tag{14}$$

$$\iiint_v \nabla(\varphi \nabla \emptyset_o - \emptyset_o \nabla \varphi) dv = \iiint_v (\varphi \nabla^2 \emptyset_o - \emptyset_o \nabla^2 \varphi) dv = 0 \tag{15}$$

So, we can obtain the Green's theorem as Equation (16) by replacing or substituting the $\nabla^2 \emptyset_o$ term with $\frac{\partial \emptyset_o}{\partial n}$ and $\nabla^2 \varphi$ with $\frac{\partial \varphi}{\partial n}$ respectively.

$$\oiint_{S_c+S_b+S_f+S_z} \left(\varphi \frac{\partial \emptyset_o}{\partial n} - \emptyset_o \frac{\partial \varphi}{\partial n}\right) ds = 0 \tag{16}$$

For marine structures, the flow field is normally bounded with the free surface, S_f and seabed boundary, S_z, together with the control surface S_c and the body surface S_b: $S_c + S_b + S_f + S_z = v$, thus for simplifying the problem, the green function must be carefully chosen as that in WAMIT (Wave Analysis MIT), as following the analysis in WAMIT, the special green function, G, can be chosen in deep water as Equation (17).

$$\emptyset_o = G\left(\vec{X}, \overrightarrow{X_o}\right) = \frac{1}{r} + \frac{1}{r'} + \frac{2k}{\pi} \int_0^\infty \frac{e^{k(z+z_O)}}{k-K} J_o(kR) dk \tag{17}$$

Where,

$k = \frac{\omega^2}{g}$

$r = \sqrt{(x-x_o)^2 + (y-y_o)^2 + (z-z_o)^2}$

r'=$\sqrt{(x-x_0)^2 + (y-y_0)^2 (z+z_0)^2}$

$R = \sqrt{(x-x_o)^2 + (y-y_o)^2}$

All these potentials and the Green's function on the body surface s_b, this is the equation we can use for solving the radiation potential φ_j. Similar to the numerical scheme for the scattering potential. We can assume the radiation potential φ_j and the normal vector component φ_j would be constants on each small panel, as such the discrete boundary integral equation for the radiation potential is given as.

$$2\pi\varphi_{jk} + \sum_{i=1(i\neq k)}^{N} \varphi_{ji} \iint_{\Delta s_i} \frac{\partial G_{ik}}{\partial n_i} ds = + \sum_{i=1(i\neq k)}^{N} n_{ji} \iint_{\Delta s_i} G_{ik} ds \tag{18}$$

j = 1, 2, 3, ……, 6
k = 1, 2, 3, ……., N

if we define the coefficient.

$a_{ik} = 0$ for i=k and $b_{ik} = 0$ for i=k

$$a_{ik} = \iint_{\Delta s_i} \frac{\partial G_{ik}}{\partial n_i} ds \; i \neq k \; \& \; b_{ik} = \iint_{\Delta s_i} G_{ik} \, ds \; for \; i \neq k \quad (19)$$

Then we can obtain the simultaneous equation for the radiation potential. This Equation (19) can be used to solve the radiation potential.

$$\begin{bmatrix} 2\pi & a_{12} & a_{13} & . & . & a_{1N} \\ a_{21} & 2\pi & a_{23} & . & . & a_{2N} \\ a_{31} & a_{32} & 2\pi & . & . & a_{3N} \\ : & : & . & . & . & . \\ a_{N1} & a_{N2} & a_{N3} & . & . & 2\pi \end{bmatrix} \begin{pmatrix} \varphi_{j1} \\ \varphi_{j2} \\ \varphi_{j3} \\ : \\ \varphi_{jN} \end{pmatrix} = \begin{bmatrix} 0 & b_{12} & b_{13} & . & . & b_{1N} \\ b_{21} & 0 & b_{23} & . & . & b_{2N} \\ b_{31} & b_{32} & 0 & . & . & b_{3N} \\ : & : & . & . & . & . \\ b_{N1} & b_{N2} & b_{N3} & . & . & 0 \end{bmatrix} \begin{pmatrix} n_{j1} \\ n_{j2} \\ n_{j3} \\ : \\ n_{jN} \end{pmatrix} \quad (20)$$

From Equation (20), it can be seen that the unit amplitude motion n_j of the structure is the forcing, thus if the forcing is zero, for instance, when the structure is fixed, the radiation potential would be zero.

Once the relevant potentials functions have been solved, the hydrostatic, hydrodynamic forces and the moments can be calculated. Which would include the hydrostatic forces, wave exciting forces, as well as the radiation force in terms of added mass and the radiation damping coefficient.

Principally, the hydrodynamic equation in time domain is actually derived from the hydrodynamic equation in Frequency domain. Since, in a linear dynamic system, we assume under the sinusoidal action, the motion would be sinusoidal accordingly, thus,

$$F_i(t) = F_i e^{-i\omega t} \quad (21)$$

While

$$x_j(t) = A_j e^{-i\omega t} \quad (22)$$

And the corresponding motion velocity and acceleration of the structure in time domain are express as Equation (23) and (24).

$$\dot{x}(t) = i\omega A_j e^{-i\omega t} \quad (23)$$

$$\ddot{x}(t) = i\omega^2 A_j e^{-i\omega t} \quad (24)$$

The time domain equation is given after applying the hydrostatic and hydrodynamic forces as Equation (25).

$$\sum_{j=1}^{6} \left(M_{ij} + a_{ij}\right) \ddot{x}_j(t) + \sum_{j=1}^{6} b_{ij} \dot{x}_j(t) + \sum_{j=1}^{6} C_{ij} x_j(t) = F_i(t) \quad (25)$$

By substituting Equation 25 becomes,

$$\sum_{j=1}^{6} \left[-\left(M_{ij} + a_{ij}\right)\omega^2 A_j + \left(b_{ij} i\omega A_j\right) + C_{ij} A_j \right] e^{-i\omega t} = F_i e^{-i\omega t} \quad (26)$$

However, we must be very careful when we transform the hydrodynamic equation in frequency domain to the equation in time domain as a_{ij}, b_{ij} and F_i are all frequency dependent.

It must be said that this linear time domain equation is only correct when the force $F_i(t)$ is sinusoidal for which the frequency of the dynamic system of the forces and the motions is well defined. However, a_{ij}, b_{ij} and F_i would become meaningless if the force $F_i(t)$ is not sinusoidal, or without a uniquely defined frequency, since in such a case, all a_{ij}, b_{ij} and F_i are uncertain.

Instead, the complete time-domain equation transformed from the frequency-domain equation is given by the expression in Equation (27).

$$\sum_{j=1}^{6} \left(M_{ij} + a_{ij}(\infty)\right) \ddot{x}_j(t) + \sum_{j=1}^{6} \int_0^t K_{ij}(t-\tau) \dot{x}_j(t) \, d\tau + \sum_{j=1}^{6} C_{ij} x_j(t) = F_i(t) \quad (27)$$

$a_{ij}(\infty)$ is the added mass at the infinite frequency, and the impulse function $K_{ij}(t)$ is a fourier transform of the radiation damping as.

$$K_{ij}(t) = \frac{2}{\pi} \int_0^{\infty} b_{ij}(\omega) \cos(\omega t) \, d\omega \quad (28)$$

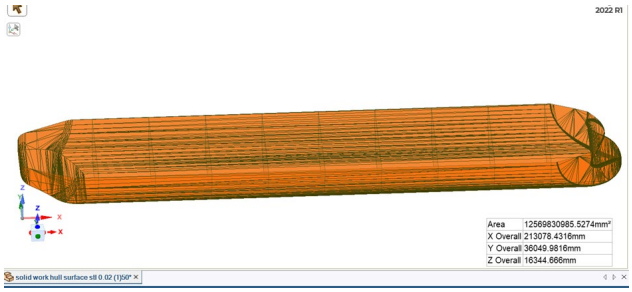

Fig. 2. Full scale model of a containership with ten bulkheads

Figure 2 depicts a 3D model of a containership hull, created in SolidWorks and saved as an STL file. The model is shown in a standard three-dimensional coordinate system, with X, Y, and Z axes clearly marked. This coordinate system is essential for any analysis of the ship's motion, as it provides a reference frame for defining position, orientation, and movement. We also see some key measurements: the total surface area of the hull is a staggering 12,569,830,985.5274 square millimeters.

This number is crucial for hydrodynamic calculations, as it directly influences the interaction between the hull and the surrounding water. The overall dimensions of the hull in the X, Y, and Z directions are also provided, giving us a sense of the ship's size and proportions. These dimensions are vital for understanding the scale of the model and for comparing it to real-world containerships. The STL file, with its detailed geometric information, serves as the foundation for any further analysis of the ship's behavior, particularly its motions in response to waves and other forces. It will be used to create a mesh, a network of interconnected elements that approximate the hull's shape, which is then used in computational methods like the Boundary Element Method. These methods allow engineers to simulate how the ship moves in different sea states, providing critical data for design and safety assessments. The accuracy of these simulations depends heavily on the quality of the STL file and the resulting mesh, highlighting the importance of precise and detailed geometric representation.

4. Results

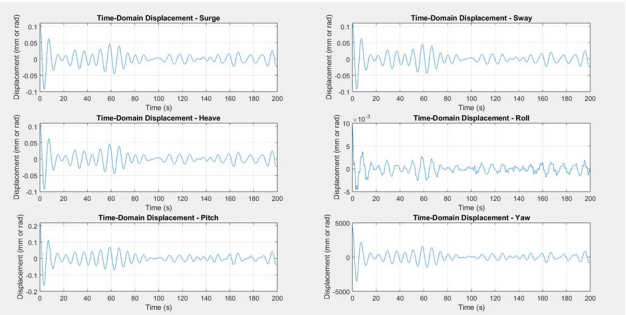

Fig. 3. Vessel displacement against time

The time-domain displacement plots for the vessel's six motion modes (surge, sway, heave, roll, pitch, and yaw) in Figure 3 provide detailed insights into the vessel's dynamic response to wave excitation, calculated using the Boundary Element Method (BEM). In surge, the displacement peaks at approximately 0.5 m before oscillating and gradually stabilizing, reflecting the vessel's forward-backward response. The sway mode shows a peak lateral displacement of around 0.1 m, indicating moderate side-to-side motion, which decays over time. The heave displacement, critical for vertical stability, peaks at about 0.5 m, similar to surge, with oscillations that gradually stabilize. In roll, displacements reach about 5×10^{-3}mm, demonstrating the rotational response about the longitudinal axis. The pitch mode exhibits displacements of approximately 3×10^{-3}mm, reflecting rotational motion about the transverse axis. Finally, yaw displacements, indicative of rotational response about the vertical axis, stabilize around 2×10^{-3}mm. These results highlight the importance of roll and pitch stabilization to maintain vessel stability, with all modes showing effective damping over time.

Figure 4 shows time-domain velocity plots for the vessel's six motion modes (surge, sway, heave, roll, pitch, and yaw), calculated using the Boundary Element Method (BEM), offer insight into the vessel's motion dynamics under wave-induced forces. In surge, the velocity peaks at approximately 0.1 m/s before oscillating and gradually stabilizing, indicating the vessel's forward-backward velocity response to wave excitation. Similarly, in sway, the velocity reaches a critical peak of 0.1 m/s, reflecting lateral motion, with oscillations damping over time. For heave, the maximum velocity is around 0.1 m/s, showing the vertical motion's response to wave loading. In roll, the velocity reaches approximately 0.5×10^{-3}rad/s, highlighting the rotational response around the longitudinal axis. The pitch velocity shows a peak of about 0.2 rad/s, indicative of the rotational response about the transverse axis. Finally, the yaw velocity exhibits a peak of approximately 2000 rad/s, representing rotational velocity about the vertical axis. These results highlight significant wave-induced motions, particularly in pitch and yaw modes, where effective stabilization is crucial to mitigate dynamic instability.

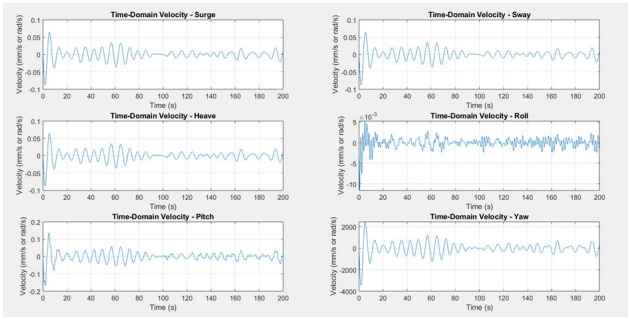

Fig. 4. Vessel velocity response against time

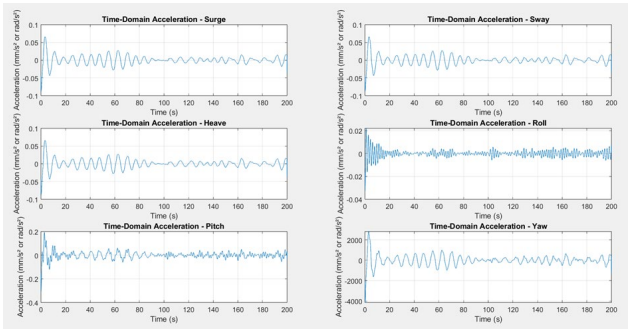

Fig. 5. Vessel acceleration response against time

The presented Figure 5 shows the vessel's acceleration response across six motion modes (surge, sway, heave, roll, pitch, and yaw) in the time domain, analyzed using the Boundary Element Method (BEM). In surge, the acceleration starts with an initial peak of approximately ±0.5 mm/s², oscillates, and stabilizes after about 80 seconds, indicating effective damping of longitudinal motions. Similarly, the sway acceleration reaches an initial amplitude of around ±0.5 mm/s² before gradually stabilizing, reflecting controlled lateral dynamics. Heave mode shows slightly lower accelerations, peaking near ±0.4 mm/s², with oscillations dampened over time, ensuring vertical motion stability. The roll acceleration is dominated by oscillations within ±0.02 rad/s², showcasing the vessel's dynamic response to rotational motions, while the pitch acceleration stabilizes around ±0.02 rad/s² after an initial spike. The yaw acceleration, with critical values peaking at ±2000 rad/s², indicates higher rotational dynamics around the vertical axis, requiring robust control mechanisms to ensure stability.

Across all modes, the trends reveal that damping mechanisms effectively reduce oscillatory responses over time, with critical values highlighting key areas for design focus.

5. Conclusion

In conclusion, a comprehensive time-domain analysis of containership motions, employing the Boundary Element Method (BEM), has yielded crucial insights into the vessel's dynamic behavior under wave excitation. Examining displacement, velocity, and acceleration across all six degrees of freedom reveals distinct characteristics for each motion mode. Surge displacement peaks at approximately 0.5m, while sway reaches around 0.1m, and heave also reaches about 0.5m, demonstrating significant translational movement. However, all three modes show effective damping. Roll and pitch displacements are considerably smaller, around $5x10^{-3}$ mm and $3x10^{-3}$ mm respectively, highlighting the importance of rotational stability. Yaw displacements stabilize around $2x10^{-3}$ mm. Velocity analysis reveals peak values of approximately 0.1 m/s for surge, sway, and heave. Rotational velocities reach approximately $0.5x10^{-3}$ rad/s for roll, 0.2 rad/s for pitch, and a substantial 2000 rad/s for yaw, indicating potentially critical rotational dynamics. Acceleration analysis shows initial peaks of approximately ±0.5 mm/s² for surge and sway, and ±0.4 mm/s² for heave, all effectively damped. Roll and pitch accelerations stabilize around ±0.02 rad/s², while yaw acceleration reaches a critical ±2000 rad/s², emphasizing the need for robust control mechanisms. These critical values, particularly the high yaw velocity and acceleration, underscore the importance of design considerations and control systems to ensure vessel stability and safe operation. The overall analysis provides valuable data for optimizing ship design and mitigating potential risks associated with wave-induced motions.

References

[1] Faltinsen, O. M. (1990). Sea Loads on Ships and Offshore Structures. Cambridge University Press.

[2] Bhattacharyya, R. (1978). Dynamics of Marine Vehicles. John Wiley & Sons.

[3] Newman, J. N. (2018). Marine Hydrodynamics (Revised Edition). MIT Press.

[4] Sheng, W., Zhang, X., Chen, W., & Wu, X. (2019). Time-domain analysis of ship motions and wave-induced loads using a nonlinear hydrodynamic approach. Applied Ocean Research, 88, 247-258.

[5] Kim, Y., & Yue, D. K. P. (1991). Theoretical and numerical study of large amplitude ship motions in time domain. International Journal of Offshore and Polar Engineering, 1(1), 16-24.

[6] Shao, Y., & Faltinsen, O. M. (2014). Time-domain simulations of fully nonlinear ship motions. Journal of Fluids and Structures, 50, 292–311.

[7] Wu, W., Kim, B. Y., & Kim, Y. (2020). A coupled CFD–BEM method for ship motion and wave load simulations. Ocean Engineering, 204, 107307.

[8] Kim, Y., Kim, J., & Shin, H. (2013). Nonlinear time-domain analysis of ship motions in severe sea states. Journal of Marine Science and Technology, 18(2), 183-195.

[9] France, W. N., Levadou, M., Treakle, T. W., Paulling, J. R., Michel, R. K., & Moore, C. (2003). Parametric rolling of containerships. SNAME Marine Technology, 40(3), 174-182.

[10] Newman, J. N. (2018). Marine Hydrodynamics (Revised Edition). MIT Press.

[11] Olusegun, S.D. & Eferebo, S.I., (2024). “Simulation of Containership Hydrodynamic Forces and Response Amplitude Operator in Time Domain”. International Journal of Engineering and Modern Technology, vol. 10, no. 11, pp. 81-91.

[12] Olusegun, S.D., Elakpa, A.A., Orji, C.U. & Tamunodukobipi, D., (2024). Simulation of a Container Vessel Using Boundary Element Method for the Computation of Hydrodynamic Pressure and Forces. International Journal of Advances in Engineering and Management, vol. 2, no. 1, pp. 50-55.